ROBUST STRAIN-TOLERANT METALLIC PHASE IN Cs-BASED HALIDE PEROVSKITE $CsAsBr_3$

Satyananda Chabungbam*[1], Nathaniel Wansuk Majaw[1], Liang Bacheng Marak[1], and Ibapyntngen Shyrkon[1]

[1]*Department of Physics, Assam Don Bosco University, Tapesia Gardens - 782402, Assam, India*

*Corresponding Author: csatya11@gmail.com

(Received 25 September 2025; revised 8 November 2025; accepted 11 November 2025; published 6 April 2026)

Abstract: Halide perovskites have emerged as a class of materials with exceptional optoelectronic properties. While most research has focused on their semiconducting nature, the exploration of metallic states in these materials is a burgeoning field. This study investigates the electronic properties of the halide perovskite $CsAsBr_3$ for the first time, which is predicted to exhibit a metallic character. Using first-principles calculations based on Density Functional Theory (DFT), we analyze the stability of this metallic state under the application of uniaxial external strain along [100] crystallographic directions. Our results demonstrate that the metallic nature of $CsAsBr_3$ is remarkably robust, persisting under both compressive and tensile strains of up to 10%. The band structure and density of states (DOS) show that the states crossing the Fermi level, primarily composed of As 4p and Br 4p orbitals, are not significantly perturbed by the applied strain. This intrinsic stability suggests that $CsAsBr_3$ is a promising candidate for flexible and strain-tolerant electronic applications where a stable metallic conductivity is required.

Keywords: Halide-Perovskites; Strain-engineering; Electronic properties
PACS: 71.15.Mb, 71.20.-b, 68.35.Gy

1 Introduction

Over the last two decades, halide perovskites, materials adopting the ABX_3 crystal structure, have transitioned from a niche academic curiosity to the forefront of materials science research [1, 2]. Their rise to prominence was ignited by the pioneering work of Kojima et al. in 2009, which demonstrated their potential in photovoltaics [3], leading to a rapid surge in power conversion efficiencies that now exceed 25% for single-junction solar cells [4]. This remarkable performance stems from a unique combination of exceptional optoelectronic properties, including strong panchromatic light absorption, long charge-carrier diffusion lengths, and high defect tolerance [5, 6]. These attributes have also made them leading candidates for a wide range of other applications, such as light-emitting diodes (LEDs), photodetectors, and thermoelectric devices [7, 8].

The archetypal halide perovskite, methylammonium lead iodide ($CH_3NH_3PbI_3$), and its inorganic counterpart, $CsPbI_3$, have been the most extensively studied [9]. However, the presence of lead (Pb) in these high-performance materials raises significant concerns regarding environmental toxicity and long-term stability, hindering their path toward widespread commercialization [10, 11]. The inherent instability of these materials in the presence of moisture, oxygen, and heat further complicates their practical application [12]. Consequently, a major thrust of current research is the exploration of lead-free halide perovskites. Several strategies have been proposed, including the use of aliovalent cation substitution to create double perovskites ($A_2B'B''X_6$) or the replacement of the divalent Pb^{2+} with other non-toxic, isoelectronic group 14 cations like Tin (Sn^{2+}) or Germanium (Ge^{2+}) [13, 14].

An alternative and compelling strategy involves replacing the divalent group 14 cation with a trivalent group 15 cation, such as Bismuth (Bi^{3+}) or Arsenic (As^{3+}) [15]. This substitution fundamentally alters the electronic configuration from a B-site ns^2 to ns^0, which can result in novel and unexpected electronic structures. While many of these trivalent cation-based systems are predicted to be semiconductors, this theoretical study have intriguingly suggested that $CsAsBr_3$ possess a metallic ground state. The emergence of metallicity in a halide perovskite is a significant departure from their conventional semiconducting character and opens a new design paradigm for this class of materials. A stable, solution-processable, and transparent metallic perovskite could find applications as a transparent conductor, potentially replacing indium tin oxide (ITO), or as a novel catalyst or thermoelectric material.

For any material to be considered for practical implementation, particularly in modern technologies like flexible or wearable electronics, its functional properties must be stable against mechanical stress and strain [16]. Strain engineering has become a powerful tool to tune the electronic properties of materials, often used to modify band gaps or induce phase transitions. However, in the context of a metallic material, it is crucial that the metallic state persists under operational strain. An unintended strain-induced metal-insulator transition would be detrimental to device performance and reliability. Therefore, understanding the response of the electronic structure of metallic $\mathrm{CsAsBr_3}$ to mechanical deformation is of both fundamental and technological importance.

This paper presents a comprehensive theoretical investigation into the stability of the metallic state in $\mathrm{CsAsBr_3}$. Using first-principles calculations, we systematically analyze the evolution of its electronic band structure and density of states under the application of uniaxial external strain. We demonstrate that the metallic nature is exceptionally robust, withstanding significant compressive and tensile strains. This finding underscores the potential of As-based perovskites as a new family of resilient metallic materials suitable for demanding electronic applications.

2 Computational Method

All first-principles calculations were performed using Density Functional Theory (DFT) [17], a powerful quantum mechanical modeling method for investigating the electronic structure of materials. We employed the Quantum ESPRESSO (version 6.8) software suite for all simulations [18, 19]. The interactions between the core and valence electrons were modeled using projector augmented-wave (PAW) pseudopotentials, which provide a balance between computational efficiency and accuracy [20]. The specific valence electron configurations considered in the pseudopotentials were Cs ($5s^2$, $5p^6$, $6s^1$), As ($4s^2$, $4p^3$), and Br ($4s^2$, $4p^5$). The exchange-correlation effects were described using the Perdew-Burke-Ernzerhof (PBE) functional, which is based on the generalized gradient approximation (GGA) [21]. This functional was chosen as it has been shown to provide reliable predictions for the structural and electronic properties of a wide range of halide perovskite systems. A kinetic energy cutoff of 50 Ry (approximately 680 eV) was applied for the plane-wave basis set to ensure convergence of the total energy. The Brillouin zone was sampled using a Monkhorst-Pack scheme with a dense 8 × 8 × 8 k-point grid for structural relaxations and self-consistent calculations [22]. To handle the occupation of electronic states near the Fermi level in this metallic system, a Gaussian smearing of 0.02 Ry was applied.

The initial crystal structure of $\mathrm{CsAsBr_3}$ was assumed to be the ideal cubic perovskite phase (space group Pm-3m, No. 221). A full geometry optimization was first performed on this unit cell, where both the lattice constant and the internal atomic positions were allowed to relax until the forces on each atom were less than 0.01 eV/Åand the total energy change between successive steps was below 10^{-5} eV. Uniaxial strain (ϵ) was subsequently applied along the $[100]$ crystallographic direction, a common method to simulate mechanical deformation in theoretical studies. The strain is defined as $\epsilon = (a - a_0)/a_0$, where 'a' is the strained lattice constant along the applied direction and '$\mathrm{a_0}$' is the fully relaxed equilibrium lattice constant from our initial optimization. The external uniaxial strain was applied to the x-direction of the unit cell at -10 % (compressive strain) to +10% (tensile strain). Finally, the electronic band structure and projected density of states (PDOS) were calculated for each relaxed, strained structure to systematically track the evolution of the electronic properties.

3 Results and Discussion

3.1 Electronic Properties of Unstrained $\mathrm{CsAsBr_3}$

First, we optimized the crystal structure of $\mathrm{CsAsBr_3}$ in its cubic perovskite phase (space group Pm-3m). The stable structure was predicted by energy minimization technique i.e. computing the lowest energy state as a function of equilibrium volume. The calculated equilibrium lattice constant was found to be 6.75 Å.

The electronic band structure and projected density of states (PDOS) for the unstrained, fully relaxed $\mathrm{CsAsBr_3}$ are shown in Figure 1 and Figure 2. The band structure clearly shows that several bands cross the Fermi level, which is a definitive signature of metallic behavior. Unlike typical semiconducting perovskites which have a distinct band gap, $\mathrm{CsAsBr_3}$ exhibits no gap, allowing for electronic conduction.

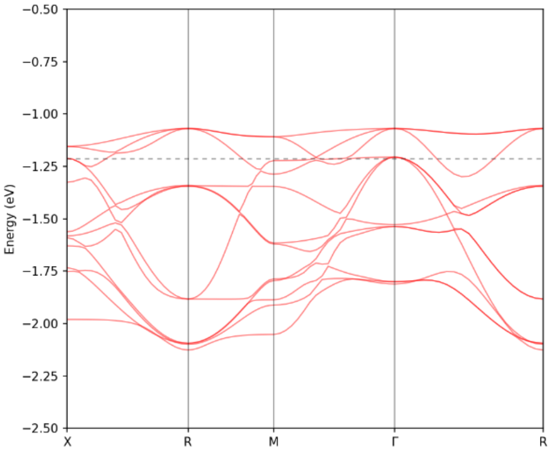

Figure 1: Bandstructure of pristine $CsAsBr_3$

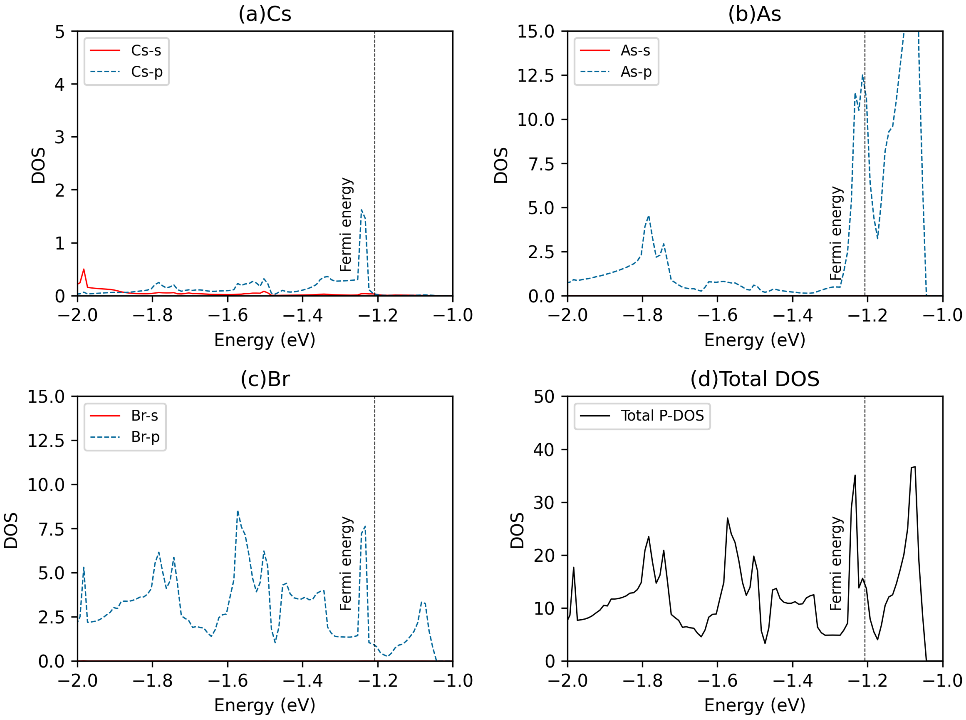

Figure 2: (a-c) PDOS and (d) DOS of pristine $CsAsBr_3$.

Analysis of the PDOS reveals the orbital contributions to the electronic states around the Fermi level. The states responsible for the metallic character arise primarily from the hybridization of As 4p and Br 4p orbitals. The conduction and valence bands are not separated, but rather overlap significantly, forming the metallic state. The Cs ions are found to have a negligible contribution to the states near the Fermi level, acting primarily as charge-donating species that stabilize the crystal structure.

3.2 Effect of Uniaxial Strain

To investigate the stability of this metallic state, we applied uniaxial strain along the [100] direction. The electronic band structures were calculated for compressive strains of -10% and tensile strains of +10%. Remarkably, the

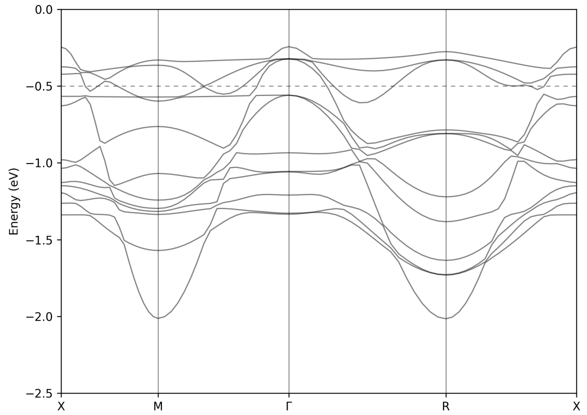

Figure 3: Bandstructure of 10% compressive strained $CsAsBr_3$

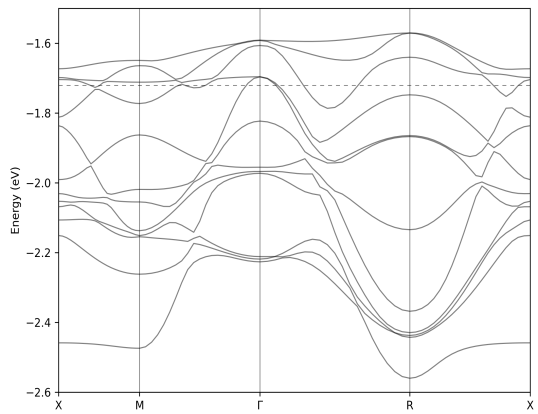

Figure 4: Bandstructure of 10% tensile strained $CsAsBr_3$

metallic character of $CsAsBr_3$ is preserved across the entire range of applied strain as shown in Figure 3 and Figure 4. In all cases, the bands continue to cross the Fermi level, indicating that a strain-induced metal-insulator transition does not occur within this range. While the applied strain does cause minor shifts in the band energies and alters their dispersion, these changes are not significant enough to open up a band gap.

Under compressive strain, the lattice constant in the applied direction is reduced, leading to increased overlap between the As 4p and Br 4p orbitals as shown in Figure 5. This slightly broadens the bands, but the fundamental metallic nature remains unchanged. Conversely, under tensile strain, the lattice is elongated, slightly reducing the orbital overlap as shown in Figure 6. This leads to a minor narrowing of the bands, but again, the overlap at the Fermi level is maintained.

The metallic conductivity arises from the strong overlap and mixing (hybridization) of the As 4p orbitals and the Br 4p orbitals.These hybridized p-orbitals form a continuous, three-dimensional (3D) framework throughout the crystal lattice. This 3D connectivity allows electrons to move freely in all directions, creating the material's metallic band structure (specifically, the Fermi level is crossed by these bands, indicating no band gap).

The robustness of the metallic state can be attributed to the intrinsic electronic structure of $CsAsBr_3$. The states at the Fermi level are derived from strong covalent interactions within the $[AsBr_3]^-$ framework. The three-dimensional nature of the perovskite structure and the p-orbital character of the relevant bands provide sufficient electronic pathways for conduction. When uniaxial strain (stretching or compression) is applied, the lattice dimensions change. However, because the electron-conducting orbitals are connected in three dimensions, the deformation along [100] axis is effectively compensated or distributed throughout the entire lattice. This strong 3D connectivity prevents the moderate lattice distortion from significantly altering the orbital overlap needed for hybridization. The p-orbital energy levels and their crossing of the Fermi level remain largely intact. Our DFT calculations essentially show that even under 10% strain, the metallic bands around the Fermi level do not separate to form a band gap. This confirms that the structural integrity of the electron-conducting channels is maintained, ensuring that the material remains metallic.

A stable, transparent, and strain-tolerant metallic perovskite like $CsAsBr_3$ is uniquely positioned for applications that require high electrical conductivity combined with mechanical flexibility and environmental durability. The most direct and high-impact application will be as a transparent conductive electrode (TCE) or charge transport layer in photovoltaic devices, addressing the limitations of existing materials like Indium Tin Oxide (ITO). Traditional ITO is brittle and cracks under strain, limiting the lifetime of flexible solar cells. $CsAsBr_3$'s stable metallic nature and strain tolerance (up to 10%) ensures the TCE maintains low resistance even when bent or stretched. It's transparency allows light to reach the active layer, crucial for high-efficiency tandem cells and transparent devices. It can also serve as the transparent, conductive layer in flexible OLEDs (Organic Light-Emitting Diodes) or capacitive touchscreens.

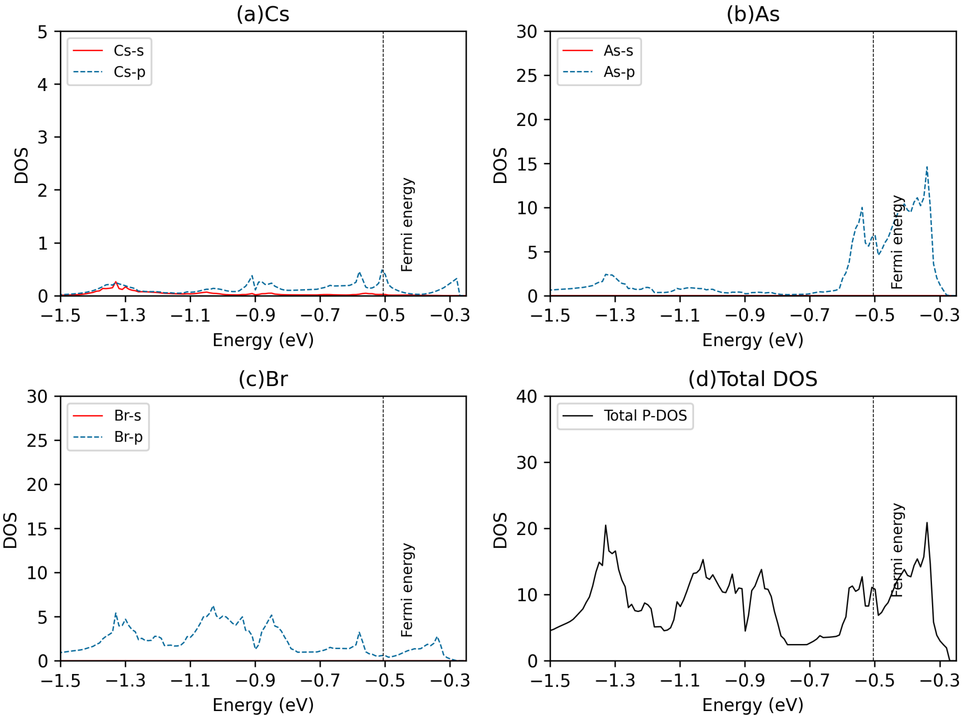

Figure 5: (a-c) pDOS and (d) DOS of 10 % compressive strained $CsAsBr_3$.

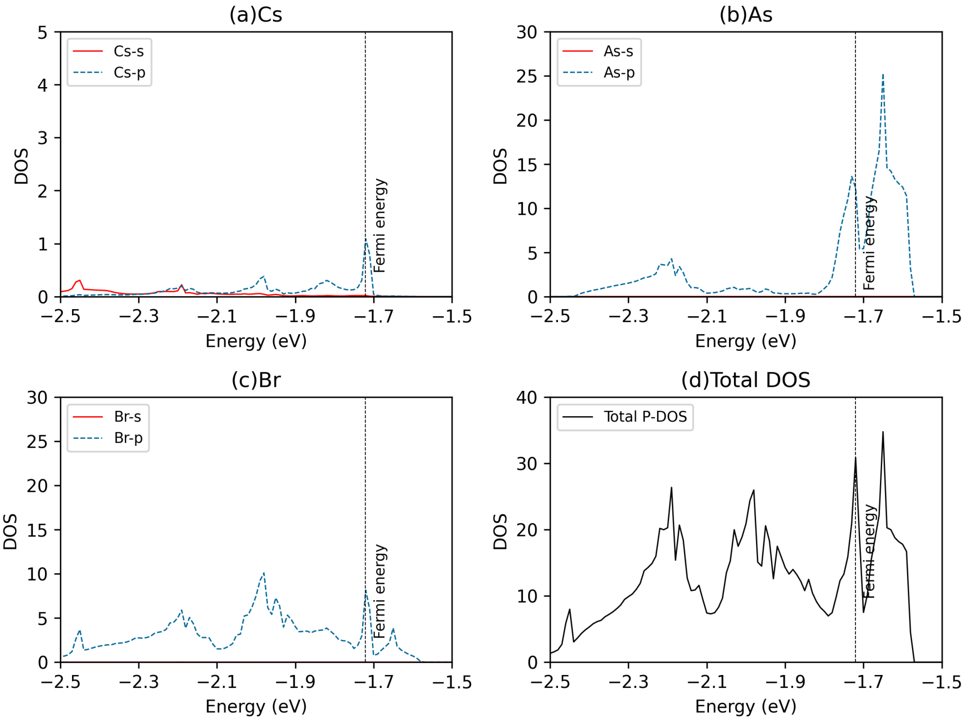

Figure 6: (a-c) pDOS and (d) DOS of 10 % tensile strained $CsAsBr_3$.

4 Conclusions

In summary, this study demonstrates through first-principles DFT calculations that the halide perovskite $CsAsBr_3$ possesses a stable metallic ground state. This metallic character, which arises from the hybridization of As 4p and Br 4p orbitals, is shown to be exceptionally robust against external uniaxial strain. The material maintains its metallic nature under both compressive and tensile strains of up to 10% applied along the [100] crystallographic direction. The resilience of the metallic state is attributed to the strong covalent framework and the three-dimensional connectivity of the electron-conducting orbitals, which are not easily disrupted by moderate lattice distortions.

The intrinsic and stable metallic nature of $CsAsBr_3$, a lead-free and relatively simple compound, makes it a highly promising material for novel electronic applications. Its robustness against mechanical strain is particularly advantageous for flexible electronics, strain sensors, and durable conductive films. This work broadens the potential functional scope of halide perovskites beyond their traditional semiconducting applications and motivates further experimental investigation into the synthesis and characterization of this intriguing class of metallic perovskites.

References

[1] M. A. Green, A. Ho-Baillie, and H. J. Snaith, Nature Photonics **8**, 506 (2014).

[2] H. J. Snaith, The Journal of Physical Chemistry Letters **4**, 3623 (2013).

[3] A. Kojima, K. Teshima, Y. Shirai, and T. Miyasaka, Journal of the American Chemical Society **131**, 6050 (2009).

[4] National Renewable Energy Laboratory (NREL), Best research-cell efficiency chart (2024).

[5] S. D. Stranks *et al.*, Science **342**, 341 (2013).

[6] R. E. Brandt, V. Stevanović, D. S. Ginley, and T. Buonassisi, MRS Communications **5**, 265 (2015).

[7] Z.-K. Tan *et al.*, Nature Nanotechnology **9**, 687 (2014).

[8] L. Dou, Y. M. Yang, J. You, and Y. Yang, Nature Communications **8**, 1470 (2017).

[9] C. C. Stoumpos, C. D. Malliakas, and M. G. Kanatzidis, Inorganic Chemistry **52**, 9019 (2013).

[10] A. Babayigit, A. Ethirajan, M. Muller, and B. Conings, Nature Materials **15**, 247 (2016).

[11] F. Giustino and H. J. Snaith, ACS Energy Letters **1**, 1233 (2016).

[12] T. Leijtens, G. E. Eperon, S. Pathak, A. Abate, M. M. Lee, and H. J. Snaith, Nature Communications **4**, 2885 (2013).

[13] Z. Xiao and Y. Yan, Advanced Energy Materials **7**, 1701136 (2017).

[14] C. C. Stoumpos *et al.*, Journal of the American Chemical Society **137**, 6804 (2015).

[15] M. R. Filip, S. Hillman, A. A. Haghighirad, H. J. Snaith, and F. Giustino, The Journal of Physical Chemistry Letters **7**, 2579 (2016).

[16] J. A. Rogers, T. Someya, and Y. Huang, Science **327**, 1603 (2010).

[17] W. Kohn and L. J. Sham, Physical Review **140**, A1133 (1965).

[18] P. Giannozzi *et al.*, Journal of Physics: Condensed Matter **21**, 395502 (2009).

[19] P. Giannozzi *et al.*, Journal of Physics: Condensed Matter **29**, 465901 (2017).

[20] P. E. Blöchl, Physical Review B **50**, 17953 (1994).

[21] J. P. Perdew, K. Burke, and M. Ernzerhof, Physical Review Letters **77**, 3865 (1996).

[22] H. J. Monkhorst and J. D. Pack, Physical Review B **13**, 5188 (1976).